Inorganic Chemistry

Article

pubs.acs.org/IC

# Lanthanide Coordination Polymers with 4,4′-Azobenzoic Acid: Enhanced Stability and Magnetocaloric Effect by Removing Guest Solvents

Shaowei Zhang, Eryue Duan, Zongsu Han, Leilei Li, and Peng Cheng*

Department of Chemistry, Key Laboratory of Advanced Energy Materials Chemistry (MOE), and Collaborative Innovation Center of Chemical Science and Engineering, Nankai University, Tianjin 300071, P. R. China

Supporting Information

**ABSTRACT:** Three lanthanide coordination polymers (Ln-CPs) formulated as $[Ln(azdc)(HCOO)]_n$ [Ln = $Gd^{III}$ (**1**), $Tb^{III}$ (**2**), $Dy^{III}$ (**3**); $H_2azdc$ = 4,4′-azobenzoic acid] have been successfully obtained by the solvothermal reaction of $Ln^{III}$ ions with $H_2azdc$ ligands in the mixed solvent *N*,*N*-dimethylformamide (DMF)/$H_2O$. Compared with our previous work on Ln-CPs with $H_2azdc$ ligands, $[Gd_2(azdc)_3(DMA)_2]_n \cdot 2n$DMA (**1′**; DMA = dimethylacetamide), in which the DMA molecules coordinate to $Gd^{III}$ ions that are replaced by $HCOO^-$ groups in **1**, resulting in the distinct structures and properties of the final products. Adjacent $Ln^{III}$ ions in **1**−**3** are connected by $HCOO^-$ groups through bridging and chelating modes to give 2D layers, which are further linked by $azdc^{2-}$ ligands to produce 3D frameworks. Magnetic results declare that antiferromagnetic couplings exist in **1**, although two different magnetic interactions among adjacent $Gd^{III}$ ions derived from antiferromagnetic interactions of the smaller Gd−O−Gd angles (Gd···Gd distances) and weak ferromagnetic interactions of the larger Gd−O−Gd angles (Gd···Gd distances) coexist in **1**. Furthermore, the magnetocaloric effect (MCE) value of **1** is 1.5 times as large as that of **1′**. More importantly, **1** exhibits excellent stabilities toward air, thermal, solvent, and acid/alkaline conditions. The results manifest that the crystalline structure of **1** can be stable at at least 425 °C supported by the in situ variable-temperature powder X-ray diffraction patterns and thermogravimetric analyses, in air for at least 3 months, and in common solvents for more than 1 week, as well as in aqueous solutions ranging from pH = 2 to 12 for more than 1 week.

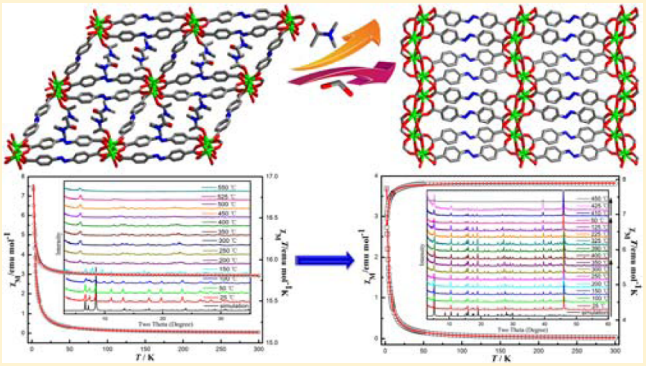

## INTRODUCTION

Coordination polymers (CPs), colloquially known as coordination compounds with repeating units extending in one, two, or three dimensions,[1] have expanded rapidly in the past 2 decades because of their intriguing structures, as well as their versatile applications in catalysis, magnetism, and fluorescent probing.[2] Compared with other metal ions, lanthanide (Ln) ions possess variable and high coordination numbers, strong spin−orbital coupling, and large magnetic moments resulting from their unique 4f electronic configurations, which impart their meaningful functionalities, such as magnetism, fluorescent sensing, magnetic resonance imaging, and others.[3] Although numerous Ln-CPs have been well-documented to date, the targeted syntheses of Ln-CPs are still an intellectual challenge because the final structures are affected not only by the starting reagents and proportions but also by the fine-tuning of the external physical and chemical changes including reaction solvents, temperature and pressure, pH value, etc.[4]

In our previous work on the exploration of Ln-CPs with the 4,4′-azobenzoic acid ($H_2azdc$) ligand, we prepared a 3D Ln-CP, $[Gd_2(azdc)_3(DMA)_2]_n \cdot 2n$DMA (**1′**; DMA = dimethylacetamide), by reacting $Gd^{III}$ ions with the $H_2azdc$ ligand in a DMA solvent.[5] The coordinated and free DMA molecules easily leave or decompose when the CP **1′** is heated, thereby leading to the destruction and collapse of the framework. We conceive that the framework would be more stable if the organic guest molecules are not contained in the targeted skeleton. Moreover, another one of our recent efforts on an exceptionally stable 3D $Gd^{III}$−organic framework containing random $Gd^{III}$ hydroxy "ladders", formulated as $\{[Gd(OH)(H_2O)(abtc)_{0.5}] \cdot H_2O\}_n$ ($H_4abtc$ = 3,3′,5,5′-azobenzenetetracarboxylic acid), has also supported the conjecture.[6]

In this contribution, we report three isostructural Ln-CPs by the solvothermal method: $[Ln(azdc)(HCOO)]_n$ [Ln = $Gd^{III}$ (**1**), $Tb^{III}$ (**2**), $Dy^{III}$ (**3**)]. In **1**−**3**, adjacent $Ln^{III}$ ions are linked by $HCOO^-$ groups via bridging and chelating modes to give 2D layers, which further generate the 3D frameworks connected by $azdc^{2-}$ ligands. Moreover, the magnetic properties of **1**−**3** have been evaluated. Importantly, as we expected, **1** displays remarkable stabilities toward air, thermal, solvent, and acid/alkaline conditions.

**Received:** April 9, 2015
**Published:** June 22, 2015





DOI: 10.1021/acs.inorgchem.5b00797
*Inorg. Chem.* 2015, 54, 6498−6503

## EXPERIMENTAL SECTION

**General Methods and Materials.** The $H_2$azdc ligand was prepared according to the previous report[7] and confirmed by $^1$H NMR. Other reagents were used as obtained. Elemental analyses (C, H, and N) were performed on a PerkinElmer 2400-II CHNS/O analyzer. Inductively coupled plasma (ICP) analyses were executed on a Thermo IRIS Advantage spectrometer. Thermogravimetric (TG) analyses were measured under a $N_2$ atmosphere on a Labsys Netzsch TG 209 Setaram apparatus with a heating rate of 10 °C·min$^{-1}$ from 25 to 800 °C. Powder X-ray diffraction (PXRD) patterns were obtained on a Rigaku Ultima IV instrument with Cu K$\alpha$ radiation ($\lambda$ = 1.54056 Å), with a scanning speed of 10°·min$^{-1}$ in the range $2\theta$ = 3−60°. The in situ variable-temperature PXRD patterns were examined on the Pt sample platform under a $N_2$ atmosphere with a heating rate of 10 °C·min$^{-1}$ from 25 to 450 °C, with a scanning speed of 5°·min$^{-1}$ in the range $2\theta$ = 3−60°. Magnetic data were gained from a Quantum Design SQUID VSM magnetometer. Diamagnetic corrections were handled with both Pascal's constants and a sample holder. The $^1$H NMR spectrum was acquired on a Mercury Vx-300 NMR spectrometer.

*Synthesis of [Gd(azdc)(HCOO)]$_n$ (**1**).* $GdCl_3·6H_2O$ (0.0372 g, 0.10 mmol), $H_2$azdc (0.0135 g, 0.05 mmol), *N*,*N*-dimethylformamide (DMF; 2.5 mL), and $H_2O$ (1.5 mL) were added in order into a 25 mL Teflon-lined stainless steel autoclave, and, subsequently, $HNO_3$ (100 $\mu$L) and 1 mol·L$^{-1}$ LiOH (100 $\mu$L) were put into the system. The mixture was kept at 140 °C for 72 h and slowly cooled to room temperature in 48 h. Orange strip crystals were collected by filtering, washed with DMF/$H_2O$, and dried in air. Yield: ca. 65% (based on $H_2$azdc). Anal. Calcd for $C_{15}H_9N_2O_6Gd$: C, 38.29; H, 1.93; N, 5.95. Found: C, 38.35; H, 2.02; N, 5.87.

*Synthesis of [Tb(azdc)(HCOO)]$_n$ (**2**).* The synthesis of **2** was similar to that of **1**, except that $TbCl_3·6H_2O$ (0.0374 g, 0.10 mmol) replaced $GdCl_3·6H_2O$. Yield: ca. 75% (based on $H_2$azdc). Anal. Calcd for $C_{15}H_9N_2O_6Tb$: C, 38.16; H, 1.92; N, 5.93. Found: C, 38.11; H, 1.98; N, 5.88.

*Synthesis of [Dy(azdc)(HCOO)]$_n$ (**3**).* The synthesis of **3** was similar to that of **1**, except that $DyCl_3·6H_2O$ (0.0377 g, 0.10 mmol) replaced $GdCl_3·6H_2O$. Yield: ca. 75% (based on $H_2$azdc). Anal. Calcd for $C_{15}H_9N_2O_6Dy$: C, 37.87; H, 1.91; N, 5.89. Found: C, 37.98; H, 1.99; N, 5.82.

**X-ray Crystallography.** Crystallographic data of **1**−**3** were collected on an Oxford SuperNova diffractometer with graphite-monochromated Mo K$\alpha$ radiation ($\lambda$ = 0.71073 Å). Routine Lorentz polarization and empirical absorption corrections were applied. All of the structures were solved by direct methods and refined by full-matrix least-squares methods on $F^2$ with the *SHELXTL-97* program package.[8] Anisotropic thermal parameters were assigned to all non-H atoms. The positions of the H atoms attached to the C and N atoms were geometrically added. The crystallographic data and structural refinements for **1**−**3** are summarized in Table 1. CCDC 1041458−1041460 are for **1**−**3**, respectively. These data can be obtained free of charge from The Cambridge Crystallographic Data Centre via www.ccdc.cam.ac.uk/data_request/cif.

## RESULTS AND DISCUSSION

**Structural Descriptions.** The experimental PXRD patterns for **1**−**3** are in good accordance with the simulated PXRD patterns from the single-crystal data, declaring high phase purity for **1**−**3** (Figure S1 in the SI).

Structural analyses suggest that **1**−**3** are isomorphous and belong to the monoclinic space group $P2_1/c$. Therefore, **1** is taken as an example to describe in detail. The asymmetric skeleton of **1** contains an eight-coordinated $Gd^{III}$ ion, one $azdc^{2-}$ ligand, and one $HCOO^-$ group (Figure 1a). It is worth noting that the HCOOH groups were generated from hydrolyzation of the DMF molecules, which was usually encountered in previous literatures.[9] The eight-coordinated Gd displays trigonal-dodecahedron geometry evaluated by the free program *SHAPE 2.0*[10] [Table S1 in the Supporting Information (SI) and Figure 1b], which is defined by four O atoms from

**Table 1. Crystallographic Data and Structure Refinements for 1−3**

| | 1 | 2 | 3 |
|---|---|---|---|
| formula | $C_{15}H_9N_2O_6Gd$ | $C_{15}H_9N_2O_6Tb$ | $C_{15}H_9N_2O_6Dy$ |
| $M_r$ (g·mol$^{-1}$) | 470.49 | 472.16 | 474.73 |
| $T$ (K) | 130.3(1) | 129.3(2) | 121.5(1) |
| cryst syst | monoclinic | monoclinic | monoclinic |
| space group | $P2(1)/c$ | $P2(1)/c$ | $P2(1)/c$ |
| $a$ (Å) | 16.7229(4) | 16.7158(4) | 16.6746(4) |
| $b$ (Å) | 12.8022(3) | 12.7707(3) | 12.7263(3) |
| $c$ (Å) | 6.8033(2) | 6.8076(2) | 6.7779(2) |
| $\beta$ (deg) | 93.670(2) | 93.669(2) | 93.634(2) |
| $V$ (Å$^3$) | 1453.52(6) | 1450.26(6) | 1435.41(6) |
| $Z$ | 4 | 4 | 4 |
| cryst size (mm$^3$) | 0.16 × 0.12 × 0.10 | 0.18 × 0.14 × 0.08 | 0.14 × 0.10 × 0.08 |
| $D_c$ (g·cm$^{-3}$) | 2.150 | 2.162 | 2.197 |
| $\mu$ (mm$^{-1}$) | 4.599 | 4.913 | 5.242 |
| $R_{int}$ | 0.0330 | 0.0410 | 0.0226 |
| limiting indices | $-18 \le h \le 19$ | $-16 \le h \le 19$ | $-19 \le h \le 19$ |
| | $-15 \le k \le 14$ | $-15 \le k \le 15$ | $-9 \le k \le 15$ |
| | $-7 \le l \le 8$ | $-5 \le l \le 8$ | $-8 \le l \le 7$ |
| reflns collected | 6108 | 5547 | 5510 |
| indep reflns | 2543 | 2543 | 2483 |
| params | 221 | 221 | 217 |
| GOF on $F^2$ | 1.059 | 1.048 | 1.150 |
| R1, wR2 [$I > 2\sigma(I)$] | 0.0223, 0.0521 | 0.0300, 0.0630 | 0.0427, 0.1017 |
| R1, wR2 (all data) | 0.0257, 0.0544 | 0.0371, 0.0686 | 0.0445, 0.1025 |

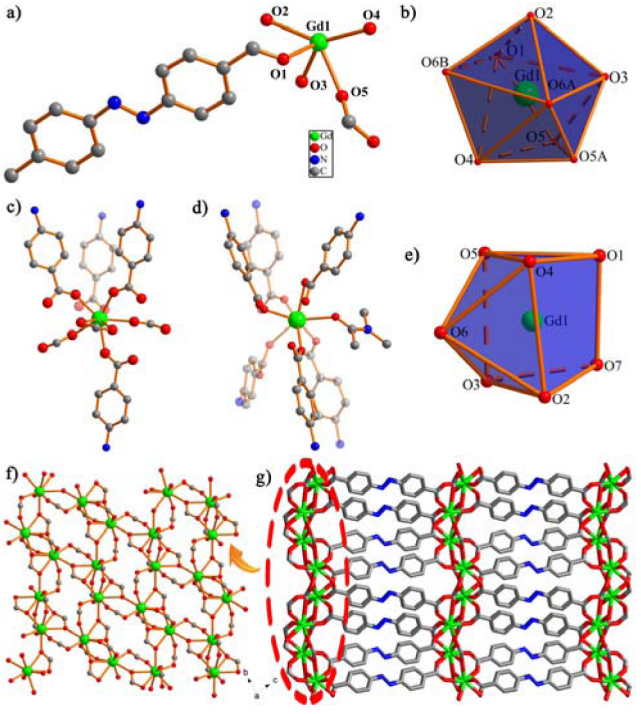


**Figure 1.** (a) Ball-and-stick representation of the molecular unit of **1**. (b and c) Coordination environment of the $Gd^{III}$ ion in **1**. (d and e) Coordination environment of the $Gd^{III}$ ion in **1′**. (f) 2D layer network constructed from the adjacent $Gd^{III}$ ions and $HCOO^-$ groups. (g) 3D framework of **1**. H atoms are omitted for clarity.



DOI: 10.1021/acs.inorgchem.5b00797
*Inorg. Chem.* 2015, 54, 6498−6503

four azdc$^{2-}$ ligands and four O atoms from three HCOO$^-$ groups with Gd−O distances of 2.281(2)−2.567(2) Å (Figure 1c). Interestingly, adjacent Gd ions are linked by HCOO$^-$ groups through bridging and chelating modes to produce the 2D layer (Figure 1f), which further form the 3D framework connected by azdc$^{2-}$ ligands (Figure 1g).

In comparison with **1′**,[5] (i) both **1** and **1′** are synthesized by solvothermal methods, which further demonstrates that the hydrothermal reaction is an effective method in constructing multidimensional CPs. (ii) Importantly, seven-coordinated Gd$^{III}$ ions in **1′** are defined by six O atoms from six azdc$^{2-}$ ligands and one DMA molecule (Figure 1d,e), which are bridged by $\mu_{1,3}$-COO groups of azdc$^{2-}$ ligands to give the 1D $[Gd_2(CO_2)_6]_n$ chain and further present the 3D fsy-type topological framework. (iii) Although the carboxyl groups of the azdc$^{2-}$ ligands in two CPs adopt the same bridging mode, there are three HCOO$^-$ groups coordinated to each Gd$^{III}$ ion in **1** so that the guest molecules cannot bind to the Gd$^{III}$ ion for steric hindrance; consequently, **1** and **1′** exhibit two distinct 3D frameworks.

**TG Analyses and in Situ Variable-Temperature PXRD.** The thermal stabilities were measured on the crystalline samples under a $N_2$ atmosphere for **1**−**3** from 25 to 800 °C (Figure S2 in the SI). The TG curves indicate that the frameworks of **1**−**3** can be stable at at least 425 °C. In order to further ensure the stability of **1**−**3**, **1** was chosen as an example to conduct the in situ variable-temperature PXRD pattern on a Pt sample platform over the temperature ranges of 25−400 and 50−450 °C (Figure 2). The corresponding PXRD patterns

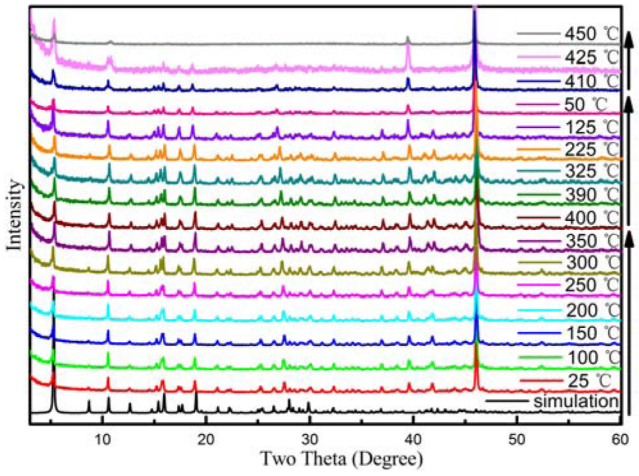


**Figure 2.** PXRD patterns simulated from the X-ray single structure of **1** and the in situ variable-temperature PXRD pattern for **1**, measured on a Pt sample platform under a $N_2$ atmosphere over the temperature ranges of 25−400 and 50−450 °C. The peaks observed at ca. 40° and 46.3° are derived from the Pt sample platform.

demonstrate that the crystalline structure of **1** remains unchanged until 425 °C, further declaring the high thermal stability of **1**. The remarkable thermal stability is extremely rare; only a few examples have been documented in previous papers,[11] to the best of our knowledge. The high thermal stability of **1** could be mainly attributed to the strong interactions among adjacent Gd$^{III}$ ions bridged by HCOO$^-$ groups, and there is no guest molecule that affects the framework when heated.

**Air and Chemical Stabilities.** When **1** was placed in the open air for 3 months, the crystal structure remained unchanged, as supported by the PXRD patterns (Figure S1 in the SI). When **1** was soaked in common solvents, such as $H_2O$, $CH_3OH$, $CH_3CH_2OH$, $CH_3CN$, $CH_2Cl_2$, acetone, DMF, DMA, dimethyl sulfoxide, tetrahydrofuran, *n*-hexane, and 1,4-dioxane for 1 week, all of the PXRD patterns were consistent with the simulated one, suggesting that **1** possesses excellent chemical stability in these solvents (Figure 3a). For evaluation

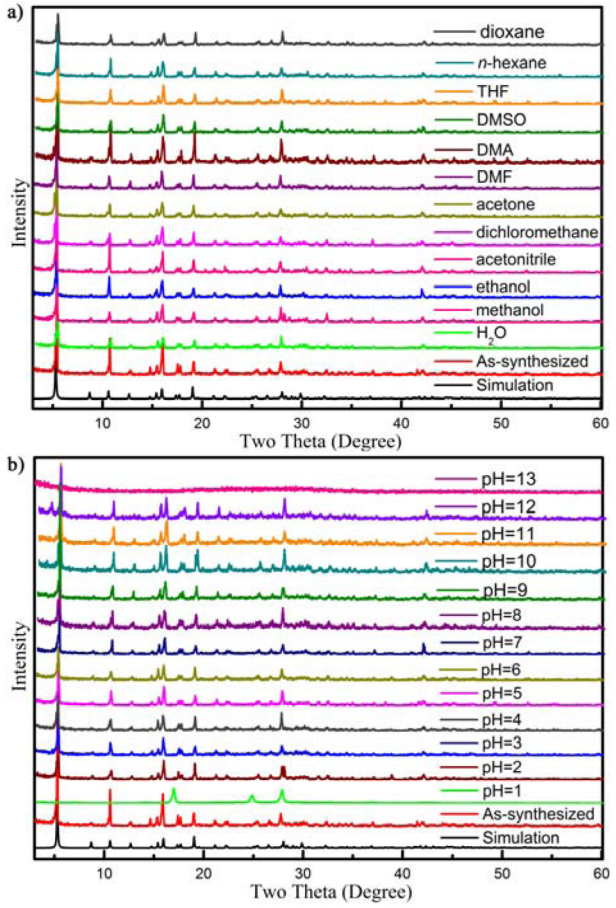


**Figure 3.** (a) PXRD patterns simulated from the single-crystal X-ray structure of **1**, as-synthesized **1**, and **1** samples placed in different solvents for 1 week. (b) PXRD patterns simulated from the single-crystal X-ray structure of **1**, as-synthesized **1**, and **1** samples soaked in aqueous solutions ranging from pH = 1 to 13 for more than 1 week.

of the acid−base resistance property of **1**, the crystal samples of **1** were immersed in the aqueous solutions ranging from pH = 1 to 13 for 1 week, respectively; the results demonstrated that the framework of **1** can be maintained in pH = 2−12 aqueous solutions for 1 week (Figure 3b). In order to further verify the stabilities of **1**, we took four representative solutions after immerssion of **1** for 1 week ($H_2O$, $CH_3OH$, pH = 2 and 12 aqueous solutions) to detect the amount of Gd$^{III}$ ions in the above filtered solutions by an ICP instrument, and the experimental results indicated that the content of Gd$^{III}$ ions in these solutions was very smal and could be ignored. The excellent stabilities of **1** may be mainly ascribed to adjacent Gd$^{III}$ ions connected by HCOO$^-$ groups through bridging/chelating modes instead of $\mu_{1,3}$-COO bridges and DMA-


DOI: 10.1021/acs.inorgchem.5b00797
*Inorg. Chem.* 2015, 54, 6498−6503

coordinated guests in **1′**, which would be conducive to improving the stability of the framework.

**Magnetic Properties.** The temperature dependencies of the magnetic susceptibilities of **1** − **3** are measured in the range of 1.8−300 K at 1000 Oe (Figures 4 and S3 in the SI). The field dependencies of the magnetization measurements at 2 K for **1**−**3** are also tested (Figure S4 in the SI).

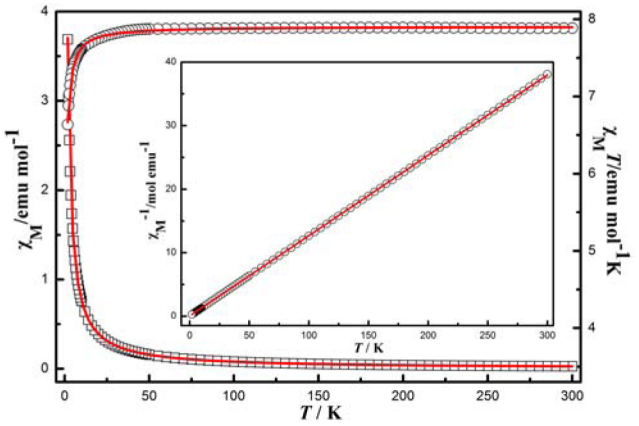


**Figure 4.** Temperature dependence of the magnetic susceptibility in the forms of $\chi_M T$ and $\chi_M$ versus $T$ for **1** at 1000 Oe between 1.8 and 300 K. The red solid lines represent the best-fitting results. Inset: Temperature dependence of the magnetic susceptibility in the form of $\chi_M^{-1}$ versus $T$ for **1** between 1.8 and 300 K. The solid line was obtained from the best fit by the Curie−Weiss expression.

In the case of **1**, $\chi_M T$ is 7.89 $cm^3 \cdot K \cdot mol^{-1}$ at 300 K, which agrees with the theoretical value of one free $Gd^{III}$ ion (7.88 $cm^3 \cdot K \cdot mol^{-1}$, $^8S_{7/2}$, $g = 2$).[12] As the temperature is decreased, $\chi_M T$ almost remains constant until to ca. 40 K and then decreases rapidly upon further cooling, reaching a minimum of 6.64 $cm^3 \cdot K \cdot mol^{-1}$ at 1.8 K (Figure 4), indicating antiferromagnetic interactions among adjacent $Gd^{III}$ ions.

As discussed in structural descriptions, neighboring $Gd^{III}$ ions are linked by $HCOO^-$ groups through bridging and chelating modes to give the 2D network in **1**; the distances for $Gd^{III} \cdots Gd^{III}$ are 3.9442(2) and 4.6118(2) Å, much shorter than the distance between adjacent 2D layers (longer than 15 Å), and the angles of Gd−O−Gd are 106.24(8) and 135.51(9)°, respectively (Figure 5). Thus, the magnetic interactions

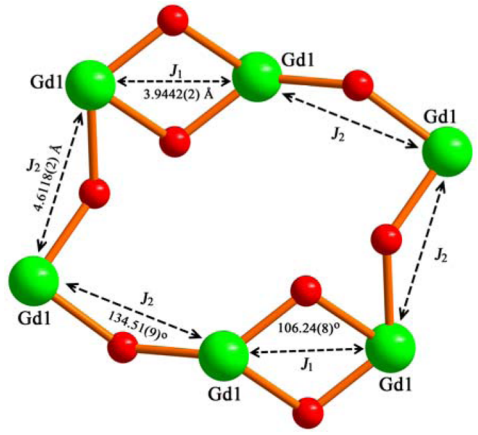


**Figure 5.** Distances among adjacent $Gd^{3+}$ ions and angles for Gd−O−Gd in **1**.

between adjacent 2D layers could be ignored and simplify analysis of the quasi-quadratic layer model, which is derived by Curély[13] (eq 1) for the isotropic Heisenberg system:

$$\chi_{2D\ square} = \frac{2Ng^2\beta^2}{3kT} \frac{S(S+1)(W_1+W_2)}{2(1-u_1^2)(1-u_2^2)} \quad (1)$$

$$W_1 = (1+u_1^2)(1+u_2^2) + 4u_1u_2$$

$$W_2 = 2u_1(1+u_2^2) + 2u_2(1+u_1^2)$$

$$u_i = \coth[J_iS(S+1)/kT] - kT/J_iS(S+1)$$

In eq 1, $N$ is Avogadro's number, $\beta$ is the Bohr magneton, $k$ is the Boltzmann constant, and $J_i$ is the exchange coupling parameter among adjacent $Gd^{III}$ ions. The best-fit parameters through eq 1 for **1** are $g = 2.004$, $J_1 = -0.120$ $cm^{-1}$, $J_2 = 0.096$ $cm^{-1}$, and $R = \sum[(\chi_M T)_{obsd} - (\chi_M T)_{calcd}]^2 / \sum[(\chi_M T)_{obsd}]^2 = 2.26 \times 10^{-4}$. Furthermore, the curve of $\chi_M^{-1}$ versus $T$ in the measured temperature range obeys the Curie−Weiss law with $C = 7.91$ $cm^3 \cdot K \cdot mol^{-1}$ and $\theta = -0.35$ K (Figure 4, inset), further proving the existence of weak antiferromagnetic interactions among adjacent $Gd^{III}$ ions in **1**.

It is worth noting that two distinct $J_i$ values are observed in adjacent $Gd^{III}$ ions, which represent that the different distances and angles among adjacent $Gd^{III}$ ions cause different magnetic interactions. In other words, ferromagnetic coupling exists among $Gd^{III}$ ions because of the presence of larger distances and angles among $Gd^{III}$ ions in **1**, which are larger than the interactions between adjacent $Gd^{III}$ ions bridged by $\mu_{1,3}$-COO groups in **1′**.[5] In contrast, antiferromagnetic interaction occurs in adjacent $Gd^{III}$ ions because of the presence of smaller distances and angles among $Gd^{III}$ ions. The $J_i$ values of the magnetic interactions could be compared with those observed for previous results on other magnetostructurally characterized carboxylate-bridged $Gd^{III}$-containing complexes (Table S1 in the SI).[12] Combining the results of **1** and previous literatures,[11] it seems that there might be a connection between the distances and angles among adjacent $Gd^{III}$ ions and magnetic couplings: the larger distances and angles among $Gd^{III}$ ions are likely to present ferromagnetic couplings; by contrast, the antiferrmagnetic interactions are usually documented among $Gd^{III}$ ions with smaller distances and angles.[12]

For **2**, the $\chi_M T$ value at 300 K is 12.06 $cm^3 \cdot K \cdot mol^{-1}$ (Figure S3a in the SI), which corresponds to the expected value for one free $Tb^{III}$ ion (11.82 $cm^3 \cdot K \cdot mol^{-1}$, $^7F_6$, $g = {}^3/_2$).[14a] As the temperature is lowered, the $\chi_M T$ value of **2** decreases slowly to 8.82 $cm^3 \cdot K \cdot mol^{-1}$ at 1.8 K. In the case of **3**, the $\chi_M T$ value 300 K is 14.17 $cm^3 \cdot K \cdot mol^{-1}$ (Figure S3b in the SI), which is consistent with the theoretical value for one free $Dy^{III}$ ion (14.17 $cm^3 \cdot K \cdot mol^{-1}$, $^6H_{15/2}$, $g = {}^4/_3$).[14a] When the temperature is lowered, the $\chi_M T$ value almost remains constant until to ca. 50 K and then decreases dramatically upon further cooling, reaching a minimum of 6.39 $cm^3 \cdot K \cdot mol^{-1}$ at 1.8 K. In addition, the curves of $\chi_M^{-1}$ versus $T$ in 1.8−300 K of **2** and **3** obey the Curie−Weiss law with negative $\theta$ values, which may be attributed to depopulation of the Stark sublevels (Figure S3 in the SI, inset).

The field-dependent magnetizations ($M$) for **1**−**3** are measured at 2 K in the range of 0−70 kG (Figure S4 in the SI). The $M$ values of **1**−**3** increase rapidly with increasing field at low fields and then steadily increase at high field, reaching the maximum values of 6.98, 5.94, and 6.66 $N\mu_B$, respectively.



DOI: 10.1021/acs.inorgchem.5b00797
Inorg. Chem. 2015, 54, 6498−6503

The maximum values of **2** and **3** are much smaller than the saturated values for noninteractive $Ln^{III}$ ions, demonstrating the presence of anisotropy and significant crystal-field effects.[14b]

The $M_W/N_{Gd}$ (where $M_W$ is the molecular mass and $N_{Gd}$ is the number of $Gd^{III}$ ions present per mole unit) value is 470.49 for **1**, which is much smaller than the value of **1′**[5] (733.83). Therefore, the MCE of **1** is evaluated by measuring the magnetization data at a field of 0.5−70 kG in the range of 2−10 K (Figure 6a), which exhibits a steady increase with increasing

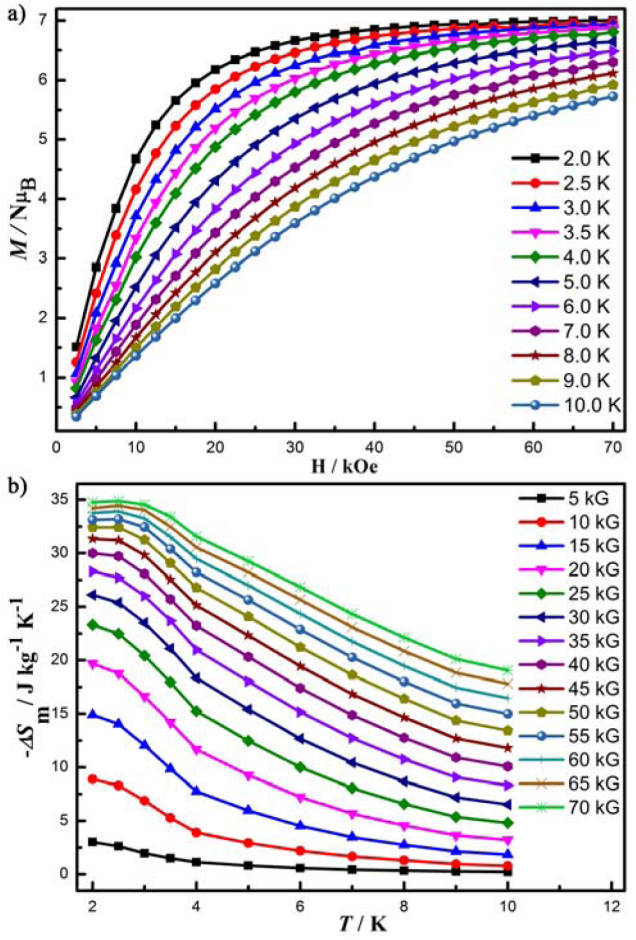


**Figure 6.** (a) Field dependencies of isothermal normalized magnetizations for **1** at $T$ = 2−10 K and 0.5−70 kG. (b) Temperature dependence of the magnetic entropy change ($-\Delta S_m$), as calculated from the magnetization data of **1** at $T$ = 2−10 K and 0.5−70 kG.

$H$ and saturation values of 6.98 N$\mu_B$ at 70 kG and 2 K, agreeing with the expected value of 7 N$\mu_B$ for one free $Gd^{III}$ ion ($S = {}^7/_2$, $g$ = 2). The magnetic entropy change $\Delta S_m$ of **1** could be obtained through the Maxwell equation (eq 2) as follows:[15]

$$\Delta S_m(T) = \int [\partial M(T, H)/\partial T]_H \, dH \quad (2)$$

In theory, the entropy value of the $Gd^{III}$ ion, calculated as $R\ln(2S + 1)$, is 17.29 J·mol$^{-1}$·K$^{-1}$. Thus, the expected entropy change value of **1** is 36.8 J·kg$^{-1}$·K$^{-1}$. The $-\Delta S_m$ value calculated from the magnetizations data is 34.9 J·kg$^{-1}$·K$^{-1}$ (75.0 mJ·cm$^{-1}$·K$^{-1}$, $D_c$ = 2.150 g·m$^{-3}$) at 2.5 K for $\Delta H$ = 70 kG (Figure 6b), being much larger than the $-\Delta S_m$ value of **1′**[5] with 22.3 J·kg$^{-1}$·K$^{-1}$ (34.9 mJ·cm$^{-1}$·K$^{-1}$), which is smaller than the calculated one because of the existence of antiferromagnetic interactions among $Gd^{III}$ ions.[16] The experimental $-\Delta S_m$ value is smaller those of than some previously prepared $Gd^{III}$-containing magnetic refrigerants, which should be ascribed to the large $M_W/N_{Gd}$ value arising from the large $H_2$azdc ligand.[16] However, the excellent stabilities of **1** toward air, solvent, and acid/alkaline conditions, especially thermostability, provide the possibility for practical application. Additionally, the $-\Delta S_m$ value per unit mass still attains a value of 26.1 J·kg$^{-1}$·K$^{-1}$ at 2.0 K for $\Delta H$ = 30 kG, which is larger than that of the commercial magnetic refrigerant (GGG), whose $-\Delta S_m$ value is 24 J·kg$^{-1}$·K$^{-1}$ ($\Delta H$ = 30 kG).[17]

## CONCLUSIONS

In summary, by the rational tuning of guest molecules based on our previous work on the $H_2$azdc ligand, three isostructural Ln-CPs have been successfully isolated, in which adjacent $Ln^{III}$ ions in **1**−**3** are connected by $HCOO^-$ groups through bridging and chelating modes to give 2D layers, further connecting the azdc$^{2-}$ ligands to generate 3D frameworks. The magnet−structure relationship of **1** has been studied in detail, and the results indicate that the magnetic interactions are closely related to the distances and angles among adjacent $Gd^{III}$ ions. Namely, there are two distinct magnetic exchanges among adjacent $Gd^{III}$ ions, resulting from weak ferromagnetic interactions of the larger Gd−O−Gd angle (Gd···Gd distances) and antiferromagnetic interactions of the smaller Gd−O−Gd angle (Gd···Gd distances) in **1**. Moreover, the MCE value of **1** is 1.5 times as large as that of **1′**. More importantly, **1** demonstrates significant stabilities toward air, thermal, solvent, and acid/alkaline conditions.

## ASSOCIATED CONTENT

### Supporting Information

PXRD patterns, TG curves, magnetic and crystallographic (in CIF format) data of **1**−**3**. The Supporting Information is available free of charge on the ACS Publications website at DOI: 10.1021/acs.inorgchem.5b00797.

## AUTHOR INFORMATION

### Corresponding Author

*E-mail: pcheng@nankai.edu.cn. Fax: (+86) 22-23502458.

### Notes

The authors declare no competing financial interest.

## ACKNOWLEDGMENTS

This work was supported by the MOST ("973 program"; Grant 2012CB821702), the NSFC (Grants 21331003 and 21421001), the MOE (Grants IRT-13022 and 13R30), the 111 project (B12015), and the NSF of Tianjin (Grant 13JCZDJC32200).

## REFERENCES

(1) Batten, S. R.; Champness, N. R.; Chen, X.-M.; Garcia-Martinez, J.; Kitagawa, S.; Öhrström, L.; O'Keeffe, M.; Paik Suh, M.; Reedijk, J. *Pure Appl. Chem.* **2013**, *85*, 1715−1724.

(2) (a) Tranchemontagne, D. J.; Mendoza-Cortes, J. L.; O'Keeffe, M.; Yaghi, O. M. *Chem. Soc. Rev.* **2009**, *38*, 1257−1283. (b) Heffern, M. C.; Matosziuk, L. M.; Meade, T. J. *Chem. Rev.* **2014**, *114*, 4496−4539. (c) Woodruff, D. N.; Winpenny, R. E. P.; Layfield, R. A. *Chem. Rev.* **2013**, *113*, 5110−5148.

(3) (a) *Lanthanide Metal−Organic Frameworks*; Cheng, P., Ed.; Springer: Berlin, 2015. (b) Liu, K.; Shi, W.; Cheng, P. *Coord. Chem. Rev.* **2015**, *289*−*290*, 74−122. (c) Lu, W.-G.; Jiang, L.; Feng, X.-L.; Lu, T.-B. *Inorg. Chem.* **2009**, *48*, 6997−6999.



DOI: 10.1021/acs.inorgchem.5b00797
*Inorg. Chem.* 2015, 54, 6498−6503

(4) For example, see: (a) Luan, X.-J.; Wang, Y.-Y.; Li, D.-S.; Liu, P.; Hu, H.-M.; Shi, Q.-Z.; Peng, S.-M. *Angew. Chem., Int. Ed.* **2005**, *44*, 3864−3867. (b) Zhang, J.; Wojtas, L.; Larsen, R. W.; Eddaoudi, M.; Zaworotko, M. J. *J. Am. Chem. Soc.* **2009**, *131*, 17040−17041. (c) Wang, X.-L.; Qin, C.; Wang, E.-B.; Li, Y.-G.; Su, Z.-M.; Xu, L.; Carlucci, L. *Angew. Chem., Int. Ed.* **2005**, *44*, 5824−5827.
(5) Zhang, S.; Shi, W.; Li, L.; Duan, E.; Cheng, P. *Inorg. Chem.* **2014**, *53*, 10340−10346.
(6) Zhang, S.; Duan, E.; Cheng, P. *J. Mater. Chem. A* **2015**, *3*, 7157−7162.
(7) Ameerunisha, S.; Zacharias, P. S. *J. Chem. Soc., Perkin Trans 2* **1995**, 1679−1682.
(8) (a) Sheldrick, G. M. *SHELXS97, Program for Crystal Structure Solution*; University of Göttingen: Göttingen, Germany, 1997. (b) Sheldrick, G. M. *SHELXL97, Program for Crystal Structure Refinement*; University of Göttingen: Göttingen, Germany, 1997.
(9) For example, see: (a) Juillard, J. *Pure Appl. Chem.* **1977**, *49*, 885−892. (b) Li, H.; Shi, W.; Zhao, K.; Niu, Z.; Chen, X.; Cheng, P. *Chem.—Eur. J.* **2012**, *18*, 5715−5723. (c) Wang, X.-Y.; Gan, L.; Zhang, S.-W.; Gao, S. *Inorg. Chem.* **2004**, *43*, 4615−4625.
(10) (a) *SHAPE: continuous shape measures calculation*, version 2.0; Electronic Structure Group, Universiat de Barcelona: Barcelona, Spain, 2010. (b) Casanova, D.; Liunell, M.; Alemany, P.; Alvarez, S. *Chem.—Eur. J.* **2005**, *11*, 1479−1494.
(11) For example, see: (a) Jiang, H.-L.; Feng, D.; Wang, K.; Gu, Z.-Y.; Wei, Z.; Chen, Y.-P.; Zhou, H.-C. *J. Am. Chem. Soc.* **2013**, *135*, 13934−13938. (b) Feng, D.; Wang, K.; Su, J.; Liu, T.-F.; Park, J.; Wei, Z.; Bosch, M.; Yakovenko, A.; Zou, X.; Zhou, H.-C. *Angew. Chem., Int. Ed.* **2015**, *54*, 149−154. (c) Gong, Y.-N.; Jiang, L.; Lu, T.-B. *Chem. Commun.* **2013**, *49*, 11113−11115.
(12) For example, see: (a) Costes, J.-P.; Clemente-Juan, J. M.; Dahan, F.; Nicodème, F.; Verelst, M. *Angew. Chem., Int. Ed.* **2002**, *41*, 323−325. (b) Hatscher, S. T.; Urland, W. *Angew. Chem., Int. Ed.* **2003**, *42*, 2862−2864. (c) Guo, F.-S.; Leng, J.-D.; Liu, J.-L.; Meng, Z.-S.; Tong, M.-L. *Inorg. Chem.* **2012**, *51*, 405−413. (d) Cañadillas-Delgado, L.; Martín, T.; Fabelo, O.; Pasán, J.; Delgado, F. S.; Lloret, F.; Julve, M.; Ruiz-Pérez, C. *Chem.—Eur. J.* **2010**, *16*, 4037−4047. (e) Randell, N. M.; Anwar, M. U.; Drover, M. W.; Dawe, L. N.; Thompson, L. K. *Inorg. Chem.* **2013**, *52*, 6731−6742. (f) Alexandropoulos, D. I.; Cunha-Silva, L.; Pham, L.; Bekiari, V.; Christou, G.; Stamatatos, T. C. *Inorg. Chem.* **2014**, *53*, 3220−3229. (g) Das, S.; Dey, A.; Biswas, S.; Colacio, E.; Chandrasekhar, V. *Inorg. Chem.* **2014**, *53*, 3417−3426.
(13) (a) Curély, J. *Europhys. Lett.* **1995**, *32*, 529. (b) Curély, J. *Phys. B* **1998**, *245*, 263−276. (c) Delgado, F. S.; Kerbellec, N.; Ruiz-Pérez, C.; Cano, J.; Lloret, F.; Julve, M. *Inorg. Chem.* **2006**, *45*, 1012−1020.
(14) (a) Aguilà, D.; Barrios, L. A.; Velasco, V.; Arnedo, L.; Aliaga-Alcalde, N.; Menelaou, M.; Teat, S. J.; Roubeau, O.; Luis, F.; Aromí, G. *Chem.—Eur. J.* **2013**, *19*, 5881−5891. (b) Hernández-Molina, M.; Ruiz-Pérez, C.; López, T.; Lloret, F.; Julve, M. *Inorg. Chem.* **2003**, *42*, 5456−5458.
(15) (a) Torres, F.; Hernández, J. M.; Bohigas, X.; Tejada, J. *Appl. Phys. Lett.* **2000**, *77*, 3248−3250. (b) Evangelisti, M.; Luis, F.; de Jongh, L. J.; Affronte, M. *J. Mater. Chem.* **2006**, *16*, 2534−2549. (c) Evangelisti, M.; Brechin, E. K. *Dalton Trans.* **2010**, *39*, 4672−4676.
(16) For example, see: (a) Chen, Y.-C.; Qin, L.; Meng, Z.-S.; Yang, D.-F.; Wu, C.; Fu, Z.; Zheng, Y.-Z.; Liu, J.-L.; Tarasenko, R.; Orendac, M.; Prokleska, J.; Sechovsky, V.; Tong, M.-L. *J. Mater. Chem. A* **2014**, *2*, 9851−9858. (b) Lorusso, G.; Sharples, J. W.; Palacios, E.; Roubeau, O.; Brechin, E. K.; Sessoli, R.; Rossin, A.; Tuna, F.; McInnes, E. J. L.; Collison, D.; Evangelisti, M. *Adv. Mater.* **2013**, *25*, 4653−4656. (c) Chen, Y.-C.; Guo, F.-S.; Zheng, Y.-Z.; Liu, J.-L.; Leng, J.-D.; Tarasenko, R.; Orendáč, M.; Prokleška, J.; Sechovský, V.; Tong, M.-L. *Chem.—Eur. J.* **2013**, *19*, 13504−13510.
(17) Daudin, B.; Lagnier, R.; Salce, B. *J. Magn. Magn. Mater.* **1982**, *27*, 315−322.



DOI: 10.1021/acs.inorgchem.5b00797
*Inorg. Chem.* 2015, 54, 6498−6503